



Evidence for Effective Multiple K^+ -Current Inhibitions by Tolvaptan, a Non-peptide Antagonist of Vasopressin V_2 Receptor

Te-Ling Lu¹, Wei-Ting Chang², Chee-Hong Chan³ and Sheng-Nan Wu^{4,5*}

¹ School of Pharmacy, China Medical University, Taichung, Taiwan, ² Division of Cardiovascular Medicine, Chi-Mei Medical Center, Tainan, Taiwan, ³ Department of Nephrology, Chang Bing Show Chwan Memorial Hospital, Changhua, Taiwan, ⁴ Department of Physiology, National Cheng Kung University Medical College, Tainan, Taiwan, ⁵ Institute of Basic Medical Sciences, National Cheng Kung University Medical College, Tainan, Taiwan

OPEN ACCESS

Edited by:

Yasuo Mori,
Kyoto University, Japan

Reviewed by:

Hiroshi Hibino,
Niigata University, Japan
Guillaume Eric Sandoz,
INSERM U1091 Institut de Biologie de
Valrose, France

*Correspondence:

Sheng-Nan Wu
snwu@mail.ncku.edu.tw

Specialty section:

This article was submitted to
Pharmacology of Ion Channels and
Channelopathies,
a section of the journal
Frontiers in Pharmacology

Received: 29 November 2018

Accepted: 21 January 2019

Published: 18 February 2019

Citation:

Lu T-L, Chang W-T, Chan C-H and
Wu S-N (2019) Evidence for Effective
Multiple K^+ -Current Inhibitions by
Tolvaptan, a Non-peptide Antagonist
of Vasopressin V_2 Receptor.
Front. Pharmacol. 10:76.
doi: 10.3389/fphar.2019.00076

Tolvaptan (TLV), an oral non-peptide antagonist of vasopressin V_2 receptor, has been increasingly used for managements in patients with hyponatremia and/or syndrome of inappropriate antidiuretic hormone secretion. However, none of the studies have thus far been investigated with regard to its possible perturbations on membrane ion currents in endocrine or neuroendocrine cells. In our electrophysiological study, the whole-cell current recordings showed that the presence of TLV effectively and differentially suppressed the amplitude of delayed rectifier K^+ ($I_{K(DR)}$) and M-type K^+ current ($I_{K(M)}$) in pituitary GH_3 cells with an IC_{50} value of 6.42 and 1.91 μM , respectively. This compound was also capable of shifting the steady-state activation curve of $I_{K(M)}$ to less depolarized potential without any appreciable change in the gating charge of this current. TLV at a concentration greater than 10 μM also suppressed the amplitude of *erg*-mediated K^+ current or the activity of large-conductance Ca^{2+} -activated K^+ channels; however, this compound failed to alter the amplitude of hyperpolarization-activated cation current in GH_3 cells. In vasopressin-preincubated GH_3 cells, TLV-mediated suppression of $I_{K(M)}$ remained little altered. Under current-clamp condition, we also observed that addition of TLV increased the firing of spontaneous action potentials in GH_3 cells and further addition of flupirtine could reverse TLV-mediated elevation of the firing. In Madin-Darby canine kidney (MDCK) cells, the K^+ current elicited by long ramp pulse was also effectively subject to inhibition by this compound. Findings from the present study were thus stated as saying that the suppression by TLV of multiple type K^+ currents could be direct and independent of its antagonism of vasopressin V_2 receptors. Our study also reveals an important aspect that should be considered when assessing aquaretic effect of TLV or its structurally similar compounds.

Keywords: tolvaptan, M-type K^+ current, delayed-rectifier K^+ current, *erg*-mediated K^+ current, membrane potential, pituitary cell, renal epithelial cell

INTRODUCTION

Tolvaptan (TLV; Samsca[®] or Jincarc[®]) is recognized as an oral aquaretic agent that functions as a selective, competitive antagonist of vasopressin V₂ receptor used to treat hyponatremia associated with congestive heart failure, cirrhosis, or the syndrome of inappropriate antidiuretic hormone (Izumi et al., 2014; Aylwin et al., 2015; Verbalis et al., 2016; Clark et al., 2017; Der-Nigoghossian et al., 2017; Dunlap et al., 2017; Felker et al., 2017; Konstam et al., 2017; Wu et al., 2017a; Berardi et al., 2018; Kogure et al., 2018; Matsukawa et al., 2018; Morris et al., 2018; Oguri et al., 2018a; Sigal et al., 2018; Takimura et al., 2018; Vidic et al., 2019). It was noted to be effective at improving the hyponatremic conditions that may occur in different pathologic conditions including that following pituitary surgery (Izumi et al., 2014; Janneck et al., 2014; Ahluwalia et al., 2015; Aylwin et al., 2015; Ichimura et al., 2015; Gralla et al., 2017; Berardi et al., 2018). Alternatively, a previous study showed the ability of the compounds recognized as the blockers of vasopressin V_{1B} receptors, to produce additional antidepressant and anxiolytic profiles (Iijima et al., 2014). TLV clinically used was also reported to improve cognitive function (Soiza and Talbot, 2011; Graziani et al., 2012; Ahluwalia et al., 2015; Verbalis et al., 2016; Der-Nigoghossian et al., 2017).

The KCNQ2, KCNQ3, and KCNQ5 genes are known to encode the core subunits of K_V7.2, K_V7.3, and K_V7.5 channels, respectively. The increased activity of these K_V channels in neuron, or endocrine or neuroendocrine cells can generate a unique population of K⁺ current, namely, the M-type K⁺ current (*I*_{K(M)}), which exhibits to possess a slowly activating and deactivating property (Brown and Yu, 2000; Quintero et al., 2005; Shu et al., 2007; Wu et al., 2012a; Hsu et al., 2014; Chen et al., 2018). Targeting *I*_{K(M)} is growingly recognized as an adjunctive regimen for the treatment of many neurological disorders. Alternatively, voltage-gated K⁺ (K_V) channels play an essential role in determining membrane excitability and the delayed rectifier K⁺ channels are ubiquitous in endocrine cells. A causal relationship between K_V3 (or KCNC) and the delayed rectifier K⁺ current (*I*_{K(DR)}) has been previously established (Rudy and McBain, 2001). The K_V3 subfamily of K_V channels is characterized by its biophysical properties exhibiting to have positively shifted voltage dependency and fast deactivation rate. These properties can be expected to limit the Na⁺ channel, thereby leading to depolarization block and accommodation of repetitive firing at high frequencies (Rudy and McBain, 2001; Tateno and Robinson, 2007). K_V channels from the K_V3.1-K_V3.2 types are the major determinants of *I*_{K(DR)} in pituitary GH₃ cells (Wang et al., 2008; So et al., 2017). However, whether TLV, expected to be a non-peptide vasopressin antagonist, exerts any perturbations on these types of K⁺ currents (e.g., *I*_{K(M)} and *I*_{K(DR)}) or on membrane potential remains largely

unexplored, although a previous report showed the ability of TLV to suppress the store-operated Ca²⁺ entry through an interaction with the Orail1 protein (Rahman and Rahman, 2017) and to increase cytosolic Ca²⁺ in Madin-Darby canine kidney (MDCK) cells (Tamma et al., 2017).

For these considerations described above, we sought to determine whether TLV or other related compounds could produce any perturbations on membrane ion channels in endocrine cells (e.g., pituitary tumor [GH₃] cells) and in renal tubular cells (e.g., MDCK cells). In particular, Ionic currents studied include *I*_{K(M)}, *I*_{K(DR)}, *erg*-mediated K⁺ current (*I*_{K(erg)}), large-conductance Ca²⁺-activated K⁺ (BK_{Ca}) channel, and hyperpolarization-activated cation current (*I*_h). Changes in membrane potential in the presence of TLV were also investigated under current-clamp condition. Unexpectedly, despite being aquaretic action, this drug at clinically relevant concentrations was capable of suppressing various types of K⁺ channels effectively in GH₃ and MDCK cells.

MATERIALS AND METHODS

Chemicals and Solution

For the present study, tolvaptan (TLV; Samsca[®] or Jincarc[®], OPC-41061, N-[4-[(7-chloro-2,3,4,5-tetrahydro-5-hydroxy-1H-1-benzazepin-1-yl)carbonyl]-3-methylphenyl]-2-methylbenzamide, C₂₆H₂₅ClN₂O₃), ivabradine and PD-118057 (2-[[4-[2-(3,4-Dichlorophenyl)ethyl]phenyl]amino]benzoic acid) were obtained from Tocris (Union Biomed Inc., Taipei, Taiwan), flupirtine, linopirdine, [Arg⁸]-vasopressin (vasopressin), nonactin, tetrodotoxin and thyrotropin releasing hormone were from Sigma-Aldrich (St Louis, MO), and pioglitazone was from Takeda Pharmaceuticals (Tokyo, Japan). The culture media, fetal bovine, calf or horse serum, L-glutamine and trypsin/EDTA were obtained from Invitrogen (Carlsbad, CA), unless stated otherwise. All other chemicals were of the highest purity commercially available, and deionized water used throughout the experiments was made from a Milli-Q water purification system (Millipore, Bedford, MA).

The composition of bath solution (i.e., normal Tyrode's solution) used in this study was 136 mM NaCl, 5.4 mM KCl, 1.8 mM CaCl₂, 0.53 mM MgCl₂, 5.5 mM glucose, and 5.5 mM HEPES-NaOH buffer, pH 7.4. To measure macroscopic K⁺ currents (e.g., *I*_{K(DR)} or *I*_h) and to preclude contamination of Cl⁻ currents, we filled the patch pipettes with a solution which contained 130 mM K-aspartate, 20 mM KCl, 1 mM KH₂PO₄, 1 mM MgCl₂, 3 mM Na₂ATP, 0.1 mM Na₂GTP, 0.1 mM EGTA, and 5 mM HEPES-KOH buffer, pH 7.2. For measurements of whole-cell *I*_{K(M)} or *I*_{K(erg)}, or single BK_{Ca}-channel activity, we used a high K⁺-bathing solution consisting of 145 mM KCl, 0.53 mM MgCl₂, and 5 mM HEPES-KOH buffer, pH 7.4, while the recording pipette used was filled with a solution containing 145 mM KCl, 2 mM MgCl₂ and 5 mM HEPES-KOH buffer, pH 7.2. The free Ca²⁺ concentration in bath medium was estimated, as the dissociation constant for EGTA and Ca²⁺ (at pH 7.2) was assumed to be 0.1 μM. For example, to provide 0.1 μM Ca²⁺, we added 0.5 mM CaCl₂ and 1 mM EGTA.

Abbreviations: AP, action potential; BK_{Ca} channel, large-conductance Ca²⁺-activated K⁺ channel; *erg*, *ether-à-go-go*-related gene; *I*-*V*, current vs. voltage; *I*_h, hyperpolarization-activated cation current; *I*_{K(DR)}, delayed-rectifier K⁺ current; *I*_{K(erg)}, *erg*-mediated K⁺ current; *I*_{K(M)}, M-type K⁺ current; K_V channel, voltage-gated K⁺ channel; MDCK cell, Madin-Darby canine kidney cell; SEM, standard error of the mean; TLV, tolvaptan.

Cell Preparations

GH₃, a clonal cell line derived from a rat prolactin-secreting pituitary tumor, was obtained from the Bioresources Collection and Research Center (BCRC-60015; Hsinchu, Taiwan). Cells were routinely cultured in Ham's F-12 medium supplemented with 15% heat-inactivated horse serum (v/v), 2.5% fetal calf serum (v/v), and 2 mM L-glutamine (Liu et al., 2009; So et al., 2017, 2018). In another separate set of experiments, we treated GH₃ cells with vasopressin (1 μM) at 37°C for 6 h. The MDCK cell line (BCRC-60004), a canine renal tubular cell line, was also obtained from the Bioresource Collection and Research Center (Hsinchu, Taiwan). MDCK cells were maintained and subcultured in Dulbecco's modified Eagle's medium supplemented with 10% fetal bovine serum (v/v) (Jan et al., 1999; Wu et al., 2015). These cells were maintained at 37°C in a humidified environment of 5% CO₂/95% air. We commonly replaced culture medium every 2 days for removal of non-adhering cells. For long-term storage, we froze the cells in culture media containing 10% dimethyl sulfoxide, and kept in liquid nitrogen. Cell viability was commonly evaluated using a WST-1 cell proliferation assay and an ELISA reader (Dynatech, Chantilly, VA).

Electrophysiological Measurements

On the day of the measurements, GH₃ or MDCK cells were dissociated, and an aliquot of cell suspension was transferred to a home-made recording chamber affixed to the stage of a DM-IL inverted microscope (Leica, Wetzlar, Germany). For visualizing change in cell size during the recordings, the microscope was coupled to a digital video system (DCR-TRV30; Sony, Japan) with a magnification of up to 1500×. The cells examined were immersed at room temperature (20–25°C) in normal Tyrode's solution, the composition of which is described above. The recording electrodes were pulled from Kimax-51 capillaries (#34500; Kimble Glass, Vineland, NJ) using either a PP-830 puller (Narishige, Tokyo, Japan) or a P-97 Flaming/Brown micropipette puller (Sutter, Novato, CA), and their tips were fire-polished with an MF-83 microforge (Narishige). The electrodes used during the recordings had a tip resistance of 3–5 MΩ when filled with different internal solution described above. Ion currents were measured in either whole-cell, cell-attached or inside-out configuration of a standard patch-clamp technique with an RK-400 (Bio-Logic, Claix, France) or an Axopatch-200B (Molecular Devices, Sunnyvale, CA) amplifier (So et al., 2017; Wu et al., 2017b). Changes in membrane potential were measured under current-clamp configuration. All potentials were commonly offset for liquid junction potentials which arose at the electrode tip when the composition of the pipette solution was different from that in the bath. Single BK_{Ca}-channel activity measured from GH₃ cells was analyzed using pCLAMP 10.2 (Molecular Devices).

Data Recordings and Analyses

The signals achieved were examined and analyzed offline using either pCLAMP 10.2 (Molecular Devices), 64-bit OriginPro 2016 (OriginLab, Northampton, MA), or custom-made macros created from Excel 2013 which was run under Windows 10 (Microsoft, Redmond, WA). Current signals were low-pass

filtered at 1 or 3 kHz. Through digital-to-analog conversion, the pCLAMP-generated voltage-step profiles with various rectangular or ramp waveforms were computer driven to evaluate either the current vs. voltage (*I-V*) relations or the steady-state activation curve for different types of ionic currents (e.g., *I*_{K(M)}) obtained with or without addition of different tested compounds.

To determine percentage inhibition of TLV on *I*_{K(M)} or *I*_{K(DR)}, we compared current amplitudes obtained in the presence of different TLV concentrations (0.1–100 μM) with the values from control experiments. To measure *I*_{K(M)}, cells were immersed in high-K⁺, Ca²⁺-free solution and, once the whole-cell current recording was achieved, each cell was depolarized from –50 to +10 mV with a duration of 1 s, while to record *I*_{K(DR)}, they were bathed in Ca²⁺-free Tyrode's solution and the depolarizing pulse from –50 to +50 mV was delivered. The concentration-dependent relationships of TLV on the inhibition of *I*_{K(M)} or *I*_{K(DR)} amplitude were fitted to a modified Hill function by nonlinear least-squares regression analysis; that is,

$$\text{Percentage inhibition (\%)} = \frac{E_{\max} \times [C]^{\eta_H}}{[C]^{\eta_H} + IC_{50}^{\eta_H}},$$

where IC₅₀ is the concentration required for a 50% inhibition, [C] the TLV concentration applied, η_H the Hill coefficient, and E_{max} maximal inhibition of *I*_{K(M)} or *I*_{K(DR)} amplitude produced by TLV.

To evaluate effect of TLV on the steady-state activation curve of *I*_{K(M)} in GH₃ cells, we held each cell at the level of –50 mV and then applied the voltage pulses from –50 to various test potentials ranging between –50 and +10 mV with a duration of 1 s which were delivered from pCLAMP 10.2 program through digital-to-analog conversion. The activation curve of the current taken with or without addition of TLV (10 μM) was fitted by the Boltzmann function:

$$\frac{I}{I_{\max}} = \frac{1}{1 + \exp[-(V - V_{1/2})qF/RT]},$$

where I_{max} is the maximal *I*_{K(M)} amplitude, V_{1/2} the voltage at which there is half-maximal activation of the current, q the apparent gating charge (i.e., the charge across the membrane electric field between closed and open conformations), R the universal gas constant, F Faraday's constant, and T the absolute temperature.

Statistical Analyses

Linear or nonlinear curve-fitting to the experimental data was appropriately implemented by using either pCLAMP 10.2 (Molecular Devices), OriginPro 2016 (OriginLab), or Microsoft Excel 2013 (i.e., "Solver" Add-in). The data are presented as mean value ± standard error of the mean (SEM) with sample sizes (n) indicating the cell number from which the results were taken; error bars are plotted as SEM. Paired or unpaired Student's *t*-tests were initially used for the statistical analyses. However, when the statistical difference among different groups was necessarily evaluated, we further implemented the *post-hoc* Duncan multiple comparisons among them. Statistical analyses

were performed using IBM SPSS version 20.0 (IBM Corp., Armonk, NY). Differences between values were considered significant when $P < 0.05$.

RESULTS

Effect of Tolvaptan (TLV) on Delayed-Rectifier K⁺ Current ($I_{K(DR)}$) in GH₃ Cells

In the first set of whole-cell experiments, we tested whether TLV had any possible perturbations on $I_{K(DR)}$ in GH₃ cells. Cells were bathed in Ca²⁺-free Tyrode's solution and the recording pipette was filled with K⁺-containing solution, the composition of which was described above. Once whole-cell mode was established, the examined cells were held at -50 mV, and the depolarizing pulse to +50 mV with a duration of 1 s was then delivered to them. Consistent with previous observations (Wang et al., 2008; So et al., 2017), the $I_{K(DR)}$ in response to such pulse protocol was drastically evoked in these cells. Unexpectedly, as cells were exposed to different concentrations of TLV, the $I_{K(DR)}$ elicited by membrane depolarization in these cells was progressively decreased (Figure 1A). For example, TLV at a concentration of 3 μ M decreased $I_{K(DR)}$ amplitude to 608 ± 16 pA from a control value of 924 ± 18 pA ($n = 12$, $P < 0.05$). After washout of this compound, current amplitude returned to 917 ± 18 pA ($n = 9$, $P < 0.05$). Figure 1B illustrates the effect of TLV (3 μ M) or linopirdine (10 μ M) on $I_{K(DR)}$ amplitude. Linopirdine is an inhibitor of M-type K⁺ currents ($I_{K(M)}$). Moreover, addition of TLV (10 μ M) was found to shorten the inactivation time constant of $I_{K(DR)}$ trajectory fitted to a monoexponential decay significantly from 687 ± 13 to 293 ± 9 ms ($n = 12$, $P < 0.05$); and, washout of the agent, time constant returned to 638 ± 11 ms ($n = 9$, $P < 0.05$) (Figure 1C). The cell diameter between the absence and presence of TLV was not noted to differ significantly (32 ± 3 μ m [in the control] vs. 31 ± 4 μ m [in the presence of 10 μ M TLV], $n = 12$, $P > 0.05$). In continued presence of 10 μ M TLV, we did not observe that subsequent application of vasopressin (1 μ M) produced any measurable effect on its suppression of $I_{K(DR)}$. However, nonactin (10 μ M), a K⁺ ionophore (Wu et al., 2012c), could reverse TLV-mediated suppression of $I_{K(DR)}$ amplitude.

Effect of TLV on $I_{K(M)}$ in GH₃ Cells

In the next set of experiments, we further explored the effect of TLV on other types of K⁺ currents (e.g., $I_{K(M)}$) inherently in these cells. We immersed the cells in high-K⁺, Ca²⁺-free solution and, during each recording, then filled the electrode with K⁺-containing solution. There are several reasons why we used high-K⁺, Ca²⁺-free solution for measurement of $I_{K(M)}$. First, removal of external Ca²⁺ in the bathing solution is to preclude the possible contamination of Ca²⁺-activated K⁺ currents in GH₃ cells. Second, the amplitude of $I_{K(M)}$ is relatively small as compared with that of $I_{K(DR)}$; however, the activation of $I_{K(M)}$ occurs near the level of resting membrane potential. Third, during cell exposure to high-K⁺, Ca²⁺-free solution at which the reversal potential is approximately zero, the potential

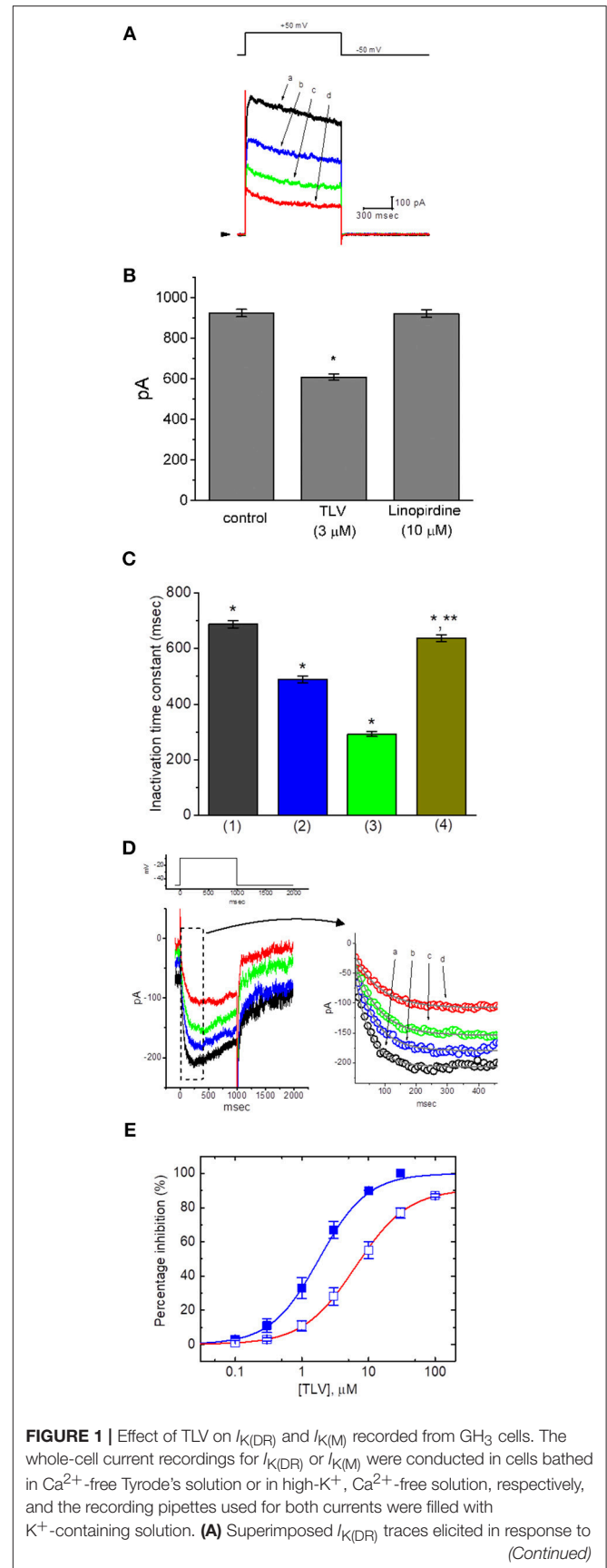


FIGURE 1 | Effect of TLV on $I_{K(DR)}$ and $I_{K(M)}$ recorded from GH₃ cells. The whole-cell current recordings for $I_{K(DR)}$ or $I_{K(M)}$ were conducted in cells bathed in Ca²⁺-free Tyrode's solution or in high-K⁺, Ca²⁺-free solution, respectively, and the recording pipettes used for both currents were filled with K⁺-containing solution. (A) Superimposed $I_{K(DR)}$ traces elicited in response to K⁺-containing solution. (Continued)

FIGURE 1 | membrane depolarization (indicated in the upper part). a: control; b: 3 μM TLV; c: 10 μM TLV; d: 30 μM TLV. Arrowhead indicates the zero current level. **(B)** Bar graph showing the effect of TLV (3 μM) or linopirdine (10 μM) on $I_{K(\text{DR})}$ amplitude in GH₃ cells (mean \pm SEM; $n = 9-12$ for each bar). *Significantly different from control ($P < 0.05$). **(C)** Bar graph showing the effect of TLV on inactivation time constant of $I_{K(\text{DR})}$ elicited by membrane depolarization (mean \pm SEM; $n = 9-12$ for each bar). 1: control; 2: 3 μM TLV; 3: 10 μM TLV; 4: washout of 10 μM TLV. *Significantly different from control ($P < 0.05$) and **significantly different from TLV (10 μM) group ($P < 0.05$). **(D)** Superimposed $I_{K(\text{M})}$ by membrane depolarization (indicated in the upper part). The upper part in **(C)** indicates the voltage protocol applied, and the right part in **(C)** is an expanded record from dashed box indicating the TLV effect on $I_{K(\text{M})}$ trajectory in the absence or presence of different TLV concentrations. a: control; b: 0.3 μM TLV, c: 1 μM TLV; d: 3 μM TLV. Each current trajectory was least-squares fitted by a single exponential (indicated by the smooth line) with the activation time constant of 49.1 ms (a; in the absence of TLV), 63.3 ms (b, 0.3 μM TLV), 72.8 ms (c, 1 μM TLV), and 80.7 ms (d, 3 μM TLV). Notably, the data points (open circles) were reduced by a factor of 10 for clarity. **(E)** Concentration-dependent relationships of TLV on $I_{K(\text{DR})}$ (\square) and $I_{K(\text{M})}$ (\blacksquare) amplitude in GH₃ cells. The relation between the percentage inhibition of $I_{K(\text{DR})}$ or $I_{K(\text{M})}$ and the TLV concentration is illustrated. Smooth curves are fits to a modified Hill function as described in section Materials and Methods. The values of IC_{50} required for inhibition of $I_{K(\text{DR})}$ and $I_{K(\text{M})}$ inherently in these cells are 6.42 and 1.91 μM , respectively, while the values for maximal suppression of those currents (i.e., E_{max}) are 91 and 100%, respectively.

applied would be near the resting membrane potential of the cells; consequently, amplified $I_{K(\text{M})}$ could be readily elicited in response to long-lasting depolarizing steps (Sankaranarayanan and Simasko, 1996). As illustrated in **Figure 1D**, when the depolarizing pulse from -50 to -10 mV was applied to the cell, a unique type of K⁺ inward current with the slowly activating and deactivating properties was readily evoked. This K⁺ current evoked in response to long-lasting membrane depolarization was subject to suppression by application of either linopirdine (10 μM) or pioglitazone (10 μM) and it has been hence identified as an $I_{K(\text{M})}$ (Sankaranarayanan and Simasko, 1996; Brown and Yu, 2000; Wu et al., 2012a; Hsu et al., 2014; Chen et al., 2018). Of particular interest, once whole-cell mode was established, as we exposed GH₃ cells to different concentrations of TLV, the $I_{K(\text{M})}$ evoked by membrane depolarization from -50 to -10 mV progressively became diminished (**Figure 1D**). For example, there was a marked reduction of current amplitude from 179 ± 10 to 94 ± 8 pA ($n = 11$, $P < 0.05$) during cell exposure to 3 μM TLV. Moreover, as cells were exposed to 3 μM TLV, the estimated activation time constant of $I_{K(\text{M})}$ in response to long membrane depolarization to -10 mV from a holding potential of -50 mV was significantly elevated to 81 ± 7 ms ($n = 11$) from a control of 49 ± 6 ms ($n = 11$, $P < 0.05$). After washout of the drug, current amplitude returned to 171 ± 9 pA ($n = 8$).

Concentration-Dependent Effects of TLV on $I_{K(\text{DR})}$ and $I_{K(\text{M})}$ in GH₃ Cells

The suppressive effects of TLV at the different concentrations, in the range of 0.1–100 μM , on $I_{K(\text{DR})}$ and $I_{K(\text{M})}$ amplitudes were further examined and compared. As depicted in **Figure 1E**, on the basis of a modified Hill function, the IC_{50} values of this compound required for the inhibitory effect of this drug on $I_{K(\text{DR})}$ and $I_{K(\text{M})}$ measured at the end of depolarizing pulse

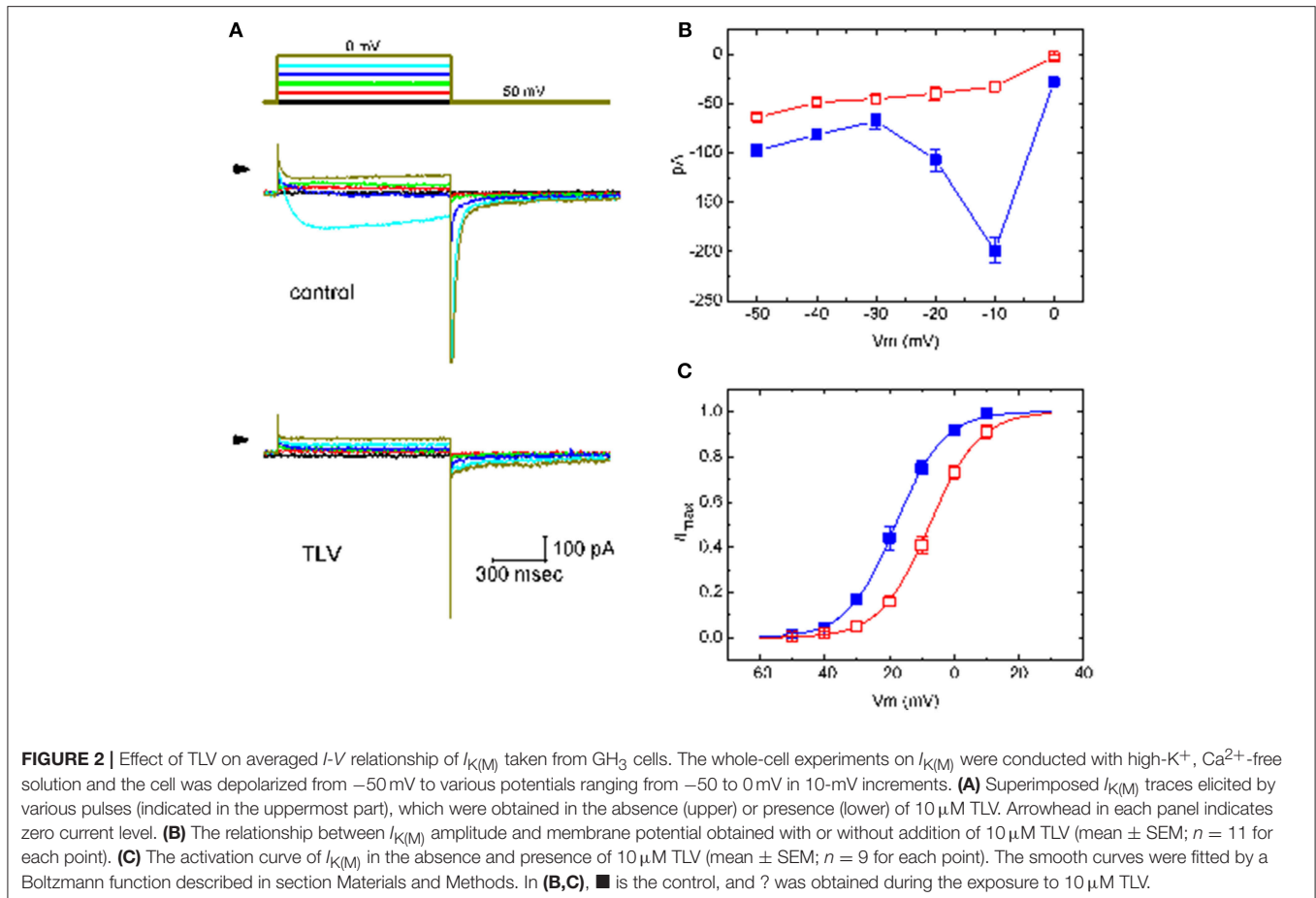
were calculated to be 6.42 and 1.91 μM , respectively, while those for maximal inhibition of these two currents were 91 and 100%, respectively. For example, TLV at a concentration of 10 μM suppressed $I_{K(\text{M})}$ amplitude by 90%, while it at the same concentration suppressed $I_{K(\text{DR})}$ amplitude only by 55%. The results would indicate, therefore, that the inhibitory effect of TLV observed in GH₃ cells was dependent on the specific types of K_v channels present.

Effect of TLV on the Steady-State Activation Curve of $I_{K(\text{M})}$ Taken From GH₃ Cells

The effect of TLV on $I_{K(\text{M})}$ elicited by different pulses from a holding potential of -50 mV was also investigated. We conducted these experiments in the cells which were immersed in high-K⁺, Ca²⁺-free solution, and the depolarizing pulses from -50 mV to various potentials were delivered to the cells. The I - V relationship for inhibitory effect of TLV (10 μM) on $I_{K(\text{M})}$ amplitude is illustrated in **Figures 2A,B**. As cells were exposed to 10 μM TLV, the whole-cell $I_{K(\text{M})}$ conductance measured at the voltage ranging between -30 and -10 mV was evidently reduced to 0.63 ± 0.04 nS ($n = 11$) from a control value of 6.57 ± 0.11 nS ($n = 11$, $P < 0.05$). The steady-state activation curve of $I_{K(\text{M})}$ in the absence or presence of TLV was further analyzed. The curves obtained with or without the addition of TLV were plotted against the test potential and satisfactorily fit to the Boltzmann equation as described under Materials and Methods (**Figure 2C**). In control (i.e., in the absence of TLV), $V_{1/2} = -18.1 \pm 1.2$ mV and $q = 3.36 \pm 0.08 e$ ($n = 11$), whereas during the exposure to TLV (10 μM), $V_{1/2} = -7.6 \pm 1.1$ mV and $q = 3.29 \pm 0.08 e$ ($n = 9$). As such, it is evident from the results that the presence of TLV not only produced a considerable reduction in $I_{K(\text{M})}$ amplitude or conductance, but it also significantly shifted the steady-state activation curve of the current to a rightward direction by approximately 10 mV. The data from these analyses showed that the translocation of around 3 e across the electric field is responsible for the voltage dependence of $I_{K(\text{M})}$ in GH₃ cells; however, minimal change in the estimated q value of the curve was detected during the exposure to TLV. Therefore, the voltage dependence of $I_{K(\text{M})}$ in these cells was virtually changed in the presence of TLV, although the movement through the electrical field in response to changes of membrane potential did not differ.

Effect of TLV on Erg-Mediated K⁺ Current ($I_{K(\text{erg})}$) in GH₃ Cells

Another type of K⁺ current (i.e., $I_{K(\text{erg})}$) functionally expressed in these cells (Wu et al., 2012b) was also further examined. To measure $I_{K(\text{erg})}$, cells were bathed in high-K⁺, Ca²⁺-free solution and the pipette was filled with K⁺-containing solution, because under such external conditions, $I_{K(\text{erg})}$ could be amplified. However, upon membrane depolarization, K⁺ currents would be overlapped with different components of K⁺ currents including $I_{K(\text{M})}$, A-type K⁺ current ($I_{K(\text{A})}$), and $I_{K(\text{DR})}$. Under experimental conditions, as the whole-cell configuration was established, the membrane hyperpolarization from -10 to -100 with a duration



of 1 s was applied to evoke $I_{K(erg)}$. As shown in **Figure 3A**, by comparison with the experimental results from the effects on $I_{K(M)}$ or $I_{K(DR)}$, the presence of TLV suppressed $I_{K(erg)}$ amplitude to a less magnitude. For example, TLV at a concentration of $10 \mu\text{M}$ slightly but significantly produced a decline in $I_{K(erg)}$ amplitude only by 8% . However, in continued presence of TLV ($30 \mu\text{M}$), further addition of PD-118057 was able to reverse the inhibition of $I_{K(erg)}$ caused by this compound, as evidenced by the elevation of $I_{K(erg)}$ amplitude from 686 ± 18 to 834 ± 19 pA ($n = 9$, $P < 0.05$) (**Figure 3B**). PD-118057 was previously reported to enhance $I_{K(erg)}$ amplitude (Zhou et al., 2005).

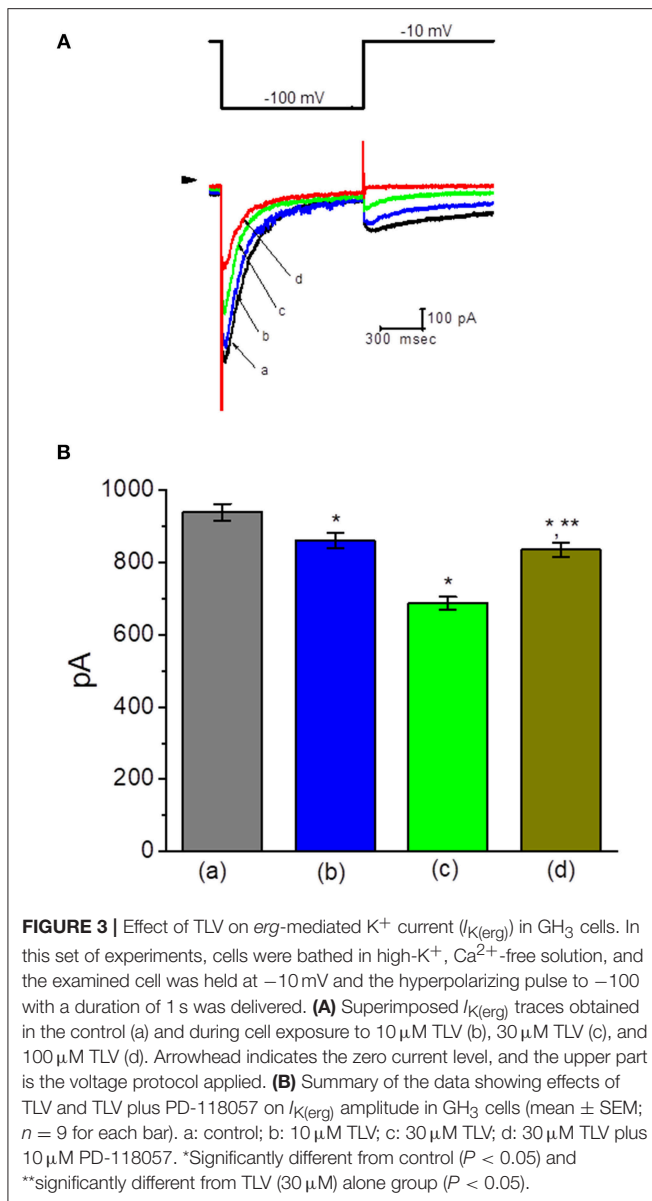
Ability of TLV to Suppress the Activity of Large-Conductance Ca^{2+} -Activated K^+ (BK_{Ca}) Channels Recorded From GH₃ Cells

We next wanted to study if TLV can alter the activity of BK_{Ca} channels enriched in GH₃ cells (Wu et al., 2004, 2017b; So et al., 2018). In these single-channel current recordings, cells were bathed in high- K^+ solution containing $0.1 \mu\text{M}$ Ca^{2+} , and each inside-out membrane patch was held at $+60$ mV. As depicted in **Figure 4**, when TLV at a concentration of $10 \mu\text{M}$ was applied to the cytosolic surface of the detached patch, the probability of BK_{Ca} channels that would be open was not changed significantly. However, addition of TLV ($30 \mu\text{M}$) was noted to reduce channel

open probability significantly, along with no clear change in single-channel amplitude, as evidenced by a reduction of channel open probability from 0.0191 ± 0.003 to 0.0143 ± 0.002 ($n = 12$, $P < 0.05$). A prolongation of mean closed time of the channel was demonstrated in the presence of TLV ($30 \mu\text{M}$) (34 ± 8 ms [control] vs. 73 ± 13 ms [in the presence of $30 \mu\text{M}$ TLV], $n = 9$, $P < 0.05$); however, the mean open time did not differ between the presence and absence of $30 \mu\text{M}$ TLV. Moreover, subsequent addition of cilostazol ($10 \mu\text{M}$), still in the presence of TLV ($30 \mu\text{M}$), effectively reversed its suppressive effect on the probability of channel openings. Cilostazol was recognized as an activator of BK_{Ca} channels (Wu et al., 2004).

Inability of TLV to Alter the Amplitude of Hyperpolarization-Activated Cation Current (I_h) Recorded From GH₃ Cells

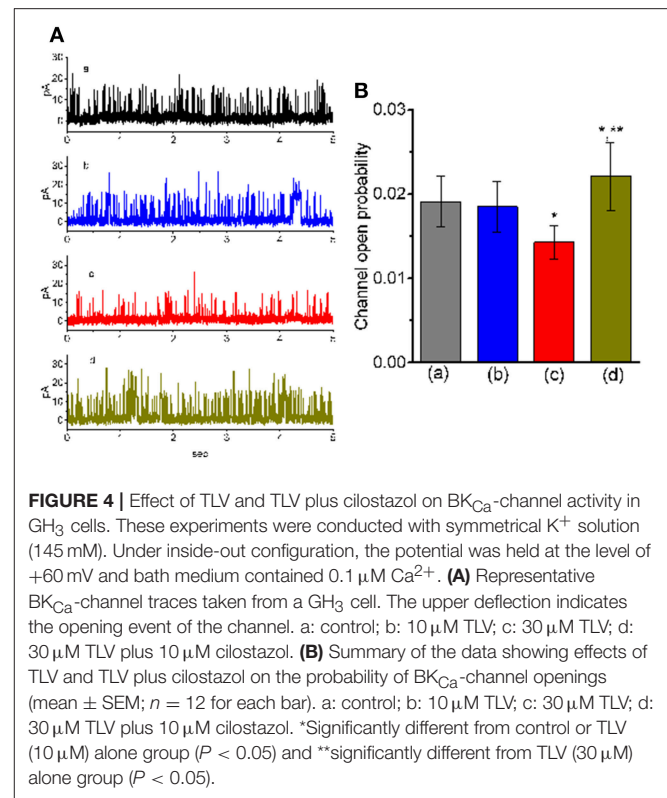
The next set of experiments was further conducted to assess if TLV could perturb the amplitude of I_h in these cells. Cells were bathed in Ca^{2+} -free Tyrode's solution containing $1 \mu\text{M}$ tetrodotoxin, and the recording electrode was filled with K^+ -containing solution. When the holding potential was clamped at -40 mV and the hyperpolarizing pulse to -100 mV with a duration of 2 s was applied, the I_h elicited under this pulse protocol was readily observed as reported previously (Liu et al.,



2009). As illustrated in **Figure 5**, the I_h amplitude elicited in response to such long-lasting membrane hyperpolarization was little changed during cell exposure to 30 μM TLV. However, further addition of ivabradine (10 μM), but still in the presence of 30 μM TLV, was effective at suppressing the amplitude of I_h , along with a considerable slowing in the activation time course of the current. Ivabradine was previously recognized as an inhibitor of I_h (Romanelli et al., 2016). Therefore, distinguishable TLV effects on $I_{K(DR)}$ or $I_{K(M)}$ as described above, the I_h amplitude in response to membrane hyperpolarization in these cells was resistant to be changed by this drug.

Effect of TLV on $I_{K(M)}$ in GH₃ Cells Preincubated With Vasopressin

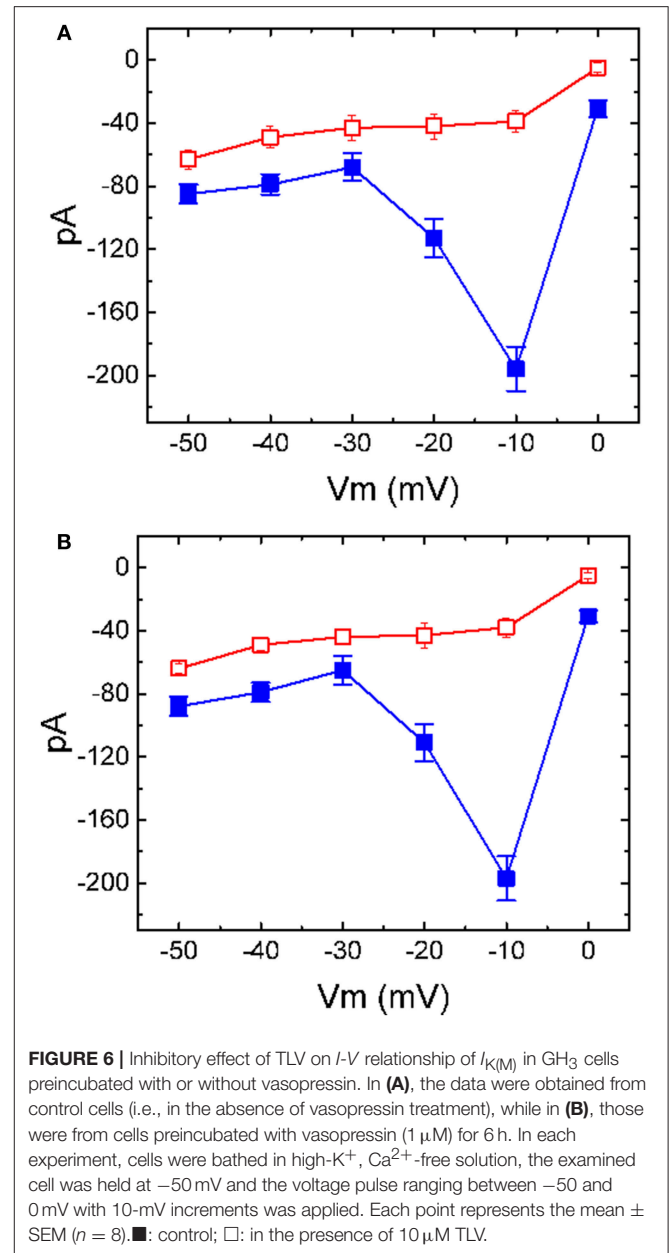
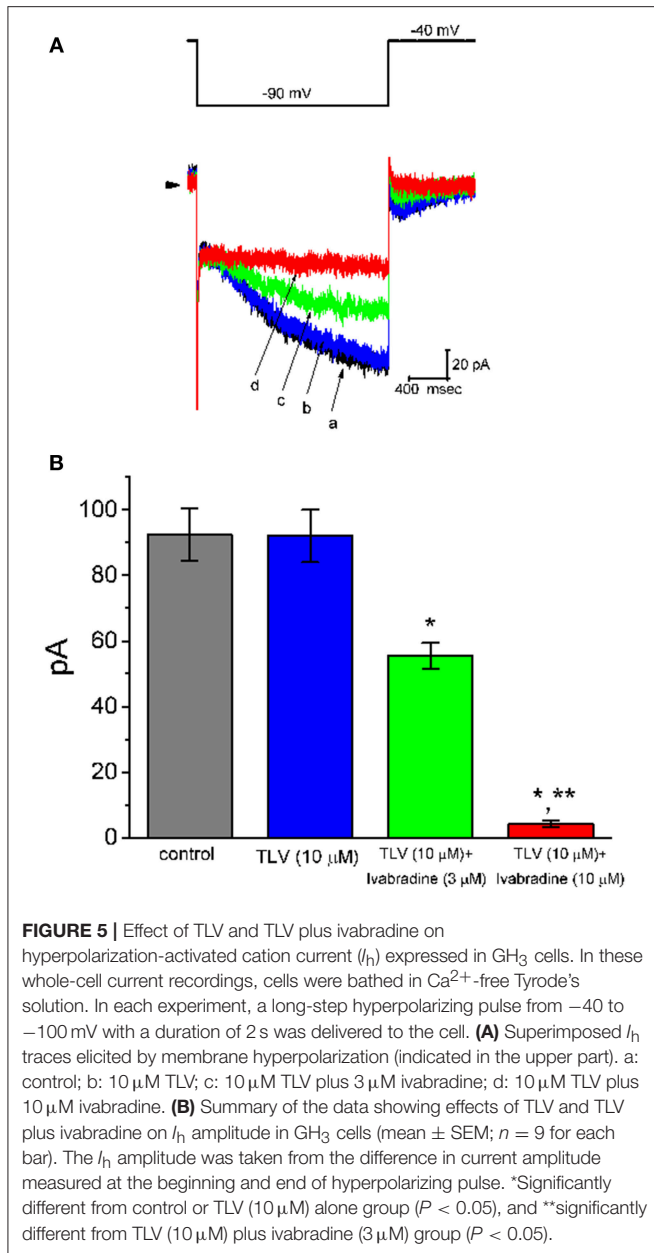
It has been shown that the effect of TLV was predominantly associated with its blockade of vasopressin receptor (Ghali et al.,



2009; Izumi et al., 2014; Clark et al., 2017; Berardi et al., 2018; Matsukawa et al., 2018). Vasopressin *per se* tends to regulate the activities of various ion channels (Nakajima et al., 1996). Moreover, the binding of vasopressin receptor by vasopressin might influence functional activities of anterior pituitary cells including GH₃ cells (Liu and Ben-Jonathan, 1994; Izumi et al., 2014). For these reasons, the effect of TLV on $I_{K(M)}$ was further evaluated in cells treated with vasopressin (1 μM) for 6 h. Of note, as compared with those effects in control cells, in GH₃ cells preincubated with vasopressin (1 μM) for 6 h, inhibitory effect of TLV on averaged $I-V$ relationship of $I_{K(M)}$ was little altered (**Figure 6**). For example, in cells pretreated with vasopressin (1 μM), addition of TLV (10 μM) evidently decreased $I_{K(M)}$ amplitude at the level of -10 mV from 197 ± 14 to 39 ± 8 pA ($n = 7$, $P < 0.05$). These results would suggest, therefore, that the observed effect of TLV on the inhibition of $I_{K(M)}$ is not solely explained by its blockade of vasopressin receptors possibly expressed in GH₃ cells.

Effect of TLV and TLV Plus Flupirtine on Spontaneous Action Potentials (APs) in GH₃ Cells

In another set of experiments, we wanted to determine whether TLV affects spontaneous APs in these cells. Cells were bathed in normal Tyrode's solution and the current-clamp voltage recordings were made to measure the occurrence of spontaneous APs. Of note, as cells were exposed to TLV, the firing of spontaneous APs was progressively elevated (**Figure 7**). For



example, TLV ($3 \mu\text{M}$) increased the firing frequency from 1.12 ± 0.05 to 1.65 ± 0.11 Hz ($n = 12$, $P < 0.05$). As we exposed GH₃ cells to TLV ($3 \mu\text{M}$), the resting potential in these cells also became significantly depolarized from -68.1 ± 0.9 to -59.2 ± 1.2 mV ($n = 12$, $P < 0.05$). Moreover, still in the presence of TLV, further application of flupirtine ($10 \mu\text{M}$), a known activator of $I_{K(M)}$ (Wu et al., 2012a), was able to reverse TLV-stimulated increase of AP firing, as evidenced by a significant reduction of firing frequency to 1.11 ± 0.06 Hz ($n = 12$, $P < 0.05$). Therefore, the results suggest that TLV-mediated changes of membrane potential in GH₃ cells ascribe largely from its inhibition of $I_{K(M)}$. Since $I_{K(M)}$ does not reach at its maximum, the increase of $I_{K(M)}$ caused by flupirtine might be responsible for its attenuation in TLV-mediated increase of the firing rate.

Effect of TLV on $I_{K(DR)}$ in Madin-Darby Canine Kidney (MDCK) Cells

Because TLV is able to exert significant function on renal epithelial cells (Tamma et al., 2017), another set of experiments was conducted in MDCK cells to determine whether this drug has any effect on $I_{K(DR)}$. The MDCK cell line has been a useful model for the investigations on functional activities in renal tubular cells (Lang and Paulmichi, 1995; Jan et al., 1999; David et al., 2013; Wu et al., 2015; Tamma et al., 2017). To evoke $I_{K(DR)}$, cells were bathed in Ca²⁺-free Tyrode's solution, the potential was held at -50 mV, and the ramp pulse from -100 to $+100$ mV with a duration of 1 s was thereafter delivered. Notably, addition of TLV suppressed $I_{K(DR)}$ amplitude effectively in these cells (Figure 8). For example, at the level of $+50$ mV, TLV ($10 \mu\text{M}$)

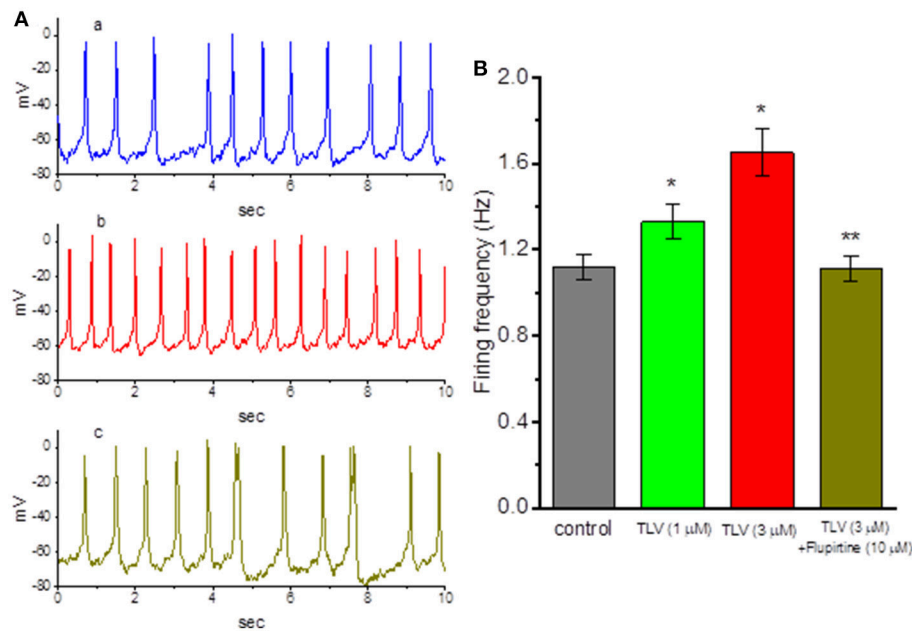


FIGURE 7 | Effects of TLV and TLV plus flupirtine on spontaneous action potentials (APs) in GH₃ cells. In these experiments conducted in whole-cell current-clamp voltage recordings, cells were bathed in normal Tyrode's solution containing 1.8 mM CaCl₂ and the recording pipette was filled with K⁺-containing solution. **(A)** Potential trace labeled a is control, and those labeled b and c were obtained after addition of 3 μM TLV and 3 μM TLV plus 10 μM flupirtine, respectively. **(B)** Summary of the data showing effects of TLV and TLV plus flupirtine on the firing frequency of spontaneous APs (mean ± SEM; *n* = 12 for each bar). *Significantly different from control (*P* < 0.05) and **significantly from TLV (3 μM) alone group (*P* < 0.05).

could significantly decrease $I_{K(DR)}$ amplitude from 121 ± 12 to 27 ± 4 pA (*n* = 9, *P* < 0.05). However, subsequent addition of vasopressin (1 μM), still in the presence of 10 μM TLV, failed to counteract the $I_{K(DR)}$ suppression by TLV.

DISCUSSION

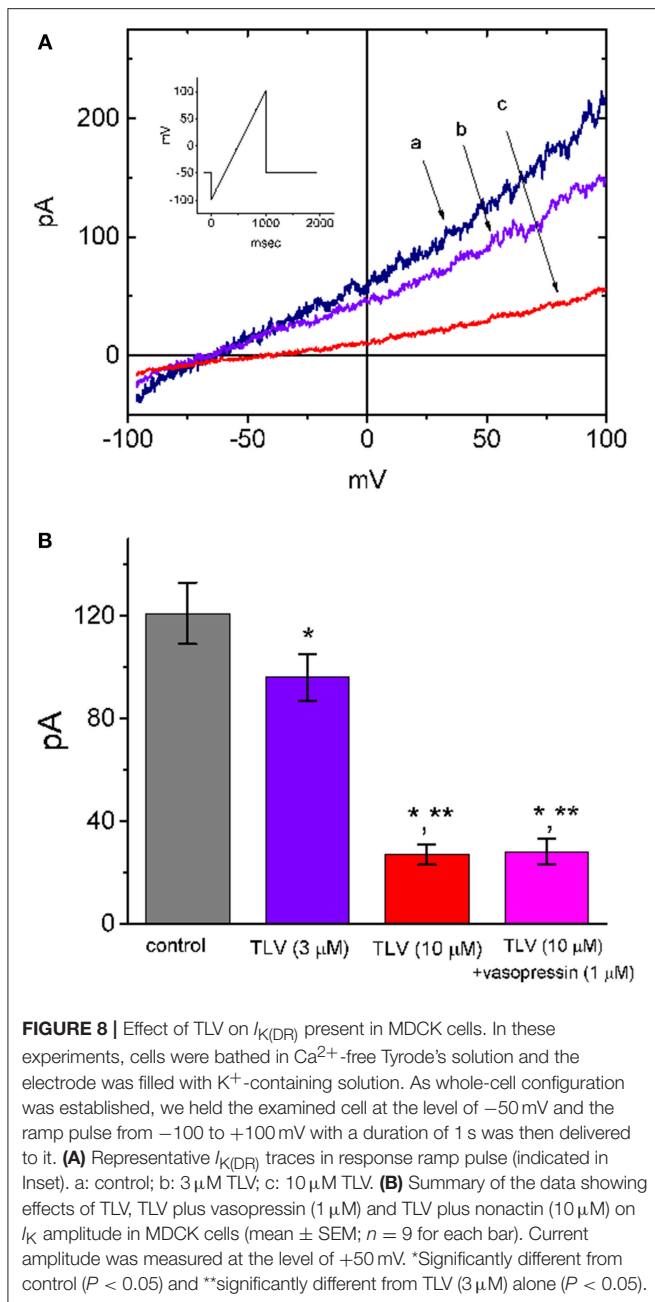
In the present study, we revealed that TLV effectively and differentially suppressed the amplitude of $I_{K(DR)}$ and $I_{K(M)}$ in a concentration- and time-dependent fashion in pituitary GH₃ cells. This drug slightly inhibited $I_{K(erg)}$ amplitude and BK_{Ca}-channel activity, while it had little or no effect on I_h . Under whole-cell voltage recordings, cell exposure to this compound was able to depolarize the membrane potential and to cause an increase in firing frequency of spontaneous APs. In MDCK cells, the presence of TLV was also effective at suppressing $I_{K(DR)}$ evoked by ramp pulse.

The IC₅₀ values of TLV needed to suppress $I_{K(DR)}$ and $I_{K(M)}$ observed in GH₃ cells were estimated to be 6.42 and 1.91 μM, respectively, indicating a 3.4-fold selectivity for its suppression of $I_{K(DR)}$ vs. $I_{K(M)}$. Additionally, our study revealed the ability of this compound to shift the steady-state activation curve of $I_{K(M)}$ to less depolarized potential, despite no measurable change in the gating charge of the curve in its presence, indicating that its presence could suppress $I_{K(M)}$ amplitude in a voltage-dependent fashion in these cells. Therefore, despite that the detailed ionic mechanisms of TLV remain to be resolved, changes in the amplitude of $I_{K(M)}$ during its exposure were rapid over

time and were sensitive to the preexistent resting potential, the concentration used, or both.

Vasopressin receptors have been previously reported to exist in anterior pituitary cells including GH₃ cells (Liu and Ben-Jonathan, 1994; Izumi et al., 2014). TLV has the propensity to interfere with the actions of vasopressin as a neurotransmitter at vasopressin receptors inherently in GH₃ cells. In our study, subsequent addition of neither vasopressin (1 μM) nor thyrotropin releasing hormone (1 μM), however, evidently reversed the suppression by TLV of $I_{K(DR)}$ or $I_{K(M)}$ seen in these cells. Moreover, in GH₃ cells preincubated with vasopressin (1 μM), the inhibitory effect of TLV on these K⁺ currents remained unaffected. Vasopressin at a concentration of 1 μM was reported to activate vasopressin receptors maximally (Armstrong et al., 2013). Therefore, findings from the present results led us to propose that the ability of TLV on suppress the amplitude of $I_{K(DR)}$, $I_{K(M)}$ or both is most likely to be independent of the mechanisms linked to either the blockade of vasopressin V₂ receptors (Ghali et al., 2009; Izumi et al., 2014; Clark et al., 2017; Berardi et al., 2018; Matsukawa et al., 2018) or the elevation in the level of intracellular inositol trisphosphate (Quintero et al., 2005).

The peak plasma concentration of TLV following single oral dose of TLV as 60-mg tablet was previously reported to reach about 720–1300 ng/ml (about 1.6–2.9 μM) (Shoaf et al., 2007). Therefore, besides the blockade of vasopressin receptor, the inhibitory effects of TLV on different types of K⁺ currents found in this study may occur within clinically therapeutic range,



and they could be a potentially important mechanism through which the drug perturbs membrane excitability of endocrine or neuroendocrine cells, if similar *in vivo* findings occur. As such, it is tempting to anticipate that both such direct inhibition of multiple K⁺ currents and blockade of vasopressin V₂ receptor by this drug or other structurally similar non-peptide compounds produce beneficial effects on patients with hyponatremia or syndrome of inappropriate antidiuretic hormone secretion.

The K_V7.1-encoded current has been notably reported to be functionally expressed in polarized MDCK cells (Jespersen et al., 2004; David et al., 2013). The suppression of K⁺ currents by TLV in renal epithelial cells could virtually exert an alternative impact on the harness of vasopressin-induced water movement.

Synergistic antagonism of vasopressin V₂ receptor and inhibition of these K⁺ currents caused by TLV at the concentrations noted to be achievable in humans (Shoaf et al., 2007; Kato et al., 2016; Oguri et al., 2018a), may also potentially account for its actions on renal epithelial cells. Therefore, determining to what extent such inhibitory actions by TLV or other structurally similar compounds (Tabata et al., 2017) contribute to their therapeutic effectiveness in renal water excretion is worthy of being imperatively investigated, as they have been rampantly used in different types of electrolyte disorders such as hyponatremia (Izumi et al., 2014; Aylwin et al., 2015; Verbalis et al., 2016; Clark et al., 2017; Der-Nigoghossian et al., 2017; Dunlap et al., 2017; Felker et al., 2017; Konstam et al., 2017; Wu et al., 2017a; Berardi et al., 2018; Kogure et al., 2018; Matsukawa et al., 2018; Morris et al., 2018; Sigal et al., 2018; Vidic et al., 2019).

Tricyclic antidepressants such as imipramine have been demonstrated to suppress various types of K⁺ currents including $I_{K(DR)}$ and $I_{K(M)}$ (Casis et al., 2002; Quintero et al., 2005). As such, whether an alternative effect on depression or anxiety disorders by the blockers of vasopressin V_{1B} receptor as described previously (Iijima et al., 2014) is linked to their possible actions on multiple types of K⁺ currents remains to be essentially resolved. Alternatively, in addition to the improvement of hyponatremic condition due to water diuresis, TLV may directly ameliorate cognitive function through a mechanism linked to its effective suppression at multiple K⁺ currents, particularly at $I_{K(M)}$, inherently in central neurons (Soiza and Talbot, 2011; Graziani et al., 2012; Ahluwalia et al., 2015; Verbalis et al., 2016; Der-Nigoghossian et al., 2017; Chen et al., 2018).

In light of the present study, despite the antagonistic effect on vasopressin V₂ receptors (Ghali et al., 2009; Izumi et al., 2014; Clark et al., 2017; Berardi et al., 2018; Matsukawa et al., 2018), our results strongly suggest that the inhibitory effects of TLV on multiple ion channels, particularly on K⁺ currents, tend to be obligate mechanisms. Through ionic mechanisms presented herein, it or other structurally similar non-peptide compounds that can be preferentially used for oral intake, is able to influence the functional activities of endocrine or renal tubular cells, if similar findings occur *in vivo*. Our findings also highlight an important alternative aspect that needs to be taken into account, inasmuch as the aquaretic effects of TLV in different pathologic disorders including polycystic kidney disease, cirrhosis or heart failure, are evaluated (Ghali et al., 2009; Graziani et al., 2012; Mancinelli et al., 2016; Clark et al., 2017; Sweeney and Avner, 2017; (Torres et al., 2017; van Gastel and Torres, 2017; Wu et al., 2017a; Chebib et al., 2018; Edwards et al., 2018; Imamura and Kinugawa, 2018; Matsukawa et al., 2018; McEwan et al., 2018; Müller et al., 2018; Oguro et al., 2018b; Poch et al., 2018; Sen et al., 2018; Takimura et al., 2018).

AUTHOR CONTRIBUTIONS

T-LL contributed to writing and experiments. W-TC contributed to experiments and materials. C-HC contributed to materials preparation and S-NW was responsible for experiment design, data collection and manuscript writing.

ACKNOWLEDGMENTS

This study was supported in part by National Cheng Kung University (D106-35A13 and NCKUH-10709001 to

S-NW), Tainan City, and by Chang Bing Show-Chwan Memorial Hospital (RD-108006 to T-LL). The authors would like to thank Kaissen Lee for contributing to part of the earlier experiments.

REFERENCES

- Ahluwalia, V., Heuman, D. M., Feldman, G., Wade, J. B., Thacker, L. R., Gavis, E., et al. (2015). Correction of hyponatremia improves, quality of life, and brain oedema in cirrhosis. *J. Hepatol.* 62, 75–82. doi: 10.1016/j.jhep.2014.07.033
- Armstrong, S. P., Seeber, R. M., Ayoub, M. A., Feldman, B. J., and Pflieger, K. D. (2013). Characterization of three vasopressin receptor 2 variants: an apparent polymorphism (V266A) and two loss-of-function mutations (R181C and M311V). *PLoS ONE* 8:e65885. doi: 10.1371/journal.pone.0065885
- Aylwin, S., Burst, V., Peri, A., Runkle, I., and Thatcher, N. (2015). ‘Dos and don’ts’ in the management of hyponatremia. *Curr. Med. Res. Opin.* 31, 1755–1761. doi: 10.1185/03007995.2015.1072706
- Berardi, R., Antonuzzo, A., Blasi, L., Buosi, R., Lorusso, V., Migliorino, M. R., et al. (2018). Practical issues for the management of hyponatremia in oncology. *Endocrine* 61, 158–164. doi: 10.1007/s12020-018-1547-y
- Brown, B. S., and Yu, S. P. (2000). Modulation and genetic identification of the M channel. *Prog. Biophys. Mol. Biol.* 73, 135–166. doi: 10.1016/S0079-6107(00)00004-3
- Casis, O., Gallego, M., and Sánchez-Chapula, J. A. (2002). Imipramine, mianserine and maprotiline block delayed rectifier potassium current in ventricular myocytes. *Pharmacol. Res.* 45, 141–146. doi: 10.1006/phrs.2002.0941
- Chebib, F. T., Perrone, R. D., Chapman, A. B., Dahl, N. K., Harris, P. C., Mrug, M., et al. (2018). A practical guide for treatment of rapidly progressive ADPKD with tolvaptan. *J. Am. Soc. Nephrol.* 29, 2458–2470. doi: 10.1681/ASN.2018060590
- Chen, T. S., Lai, M. C., Hung, T. Y., Lin, K. M., Huang, C. W., and Wu, S. N. (2018). Pioglitazone, a PPAR- γ activator, stimulates BK_{Ca} but suppresses IK_m in hippocampal neurons. *Front. Pharmacol.* 9:977. doi: 10.3389/fphar.2018.00977
- Clark, W. F., Devuyt, O., and Roussel, R. (2017). The vasopressin system: new insights for patients with kidney diseases: epidemiological evidence and therapeutic perspectives. *J. Intern. Med.* 282, 310–321. doi: 10.1111/joim.12654
- David, J. P., Andersen, M. N., Olesen, S. P., Rasmussen, H. B., and Schmitt, N. (2013). Trafficking of the IKs-complex in MDCK cells: site of subunit assembly and determinants of polarized localization. *Traffic* 14, 399–411. doi: 10.1111/tra.12042
- Der-Nigoghossian, C., Lesch, C., and Berger, K. (2017). Effectiveness and tolerability of conivaptan and tolvaptan for the treatment of hyponatremia in neurocritically III patients. *Pharmacotherapy* 37, 528–534. doi: 10.1002/phar.1926
- Dunlap, M. E., Hauptman, P. J., Amin, A. N., Chase, S. L., Chiodo, J. A., Chiong, J. R., et al. (2017). Current management of hyponatremia in acute heart failure: a report from the hyponatremia registry for patients with euvoletic and hypervolemic hyponatremia (HN registry). *J. Am. Heart Assoc.* 6:e005261. doi: 10.1161/JAHA.116.005261
- Edwards, M. E., Chebib, F. T., Irazabal, M. V., Ofstie, T. G., Bungum, L. A., Metzger, A. J., et al. (2018). Long-term administration of tolvaptan in autosomal dominant polycystic kidney disease. *Clin. J. Am. Soc. Nephrol.* 13, 1153–1161. doi: 10.2215/CJN.01520218
- Felker, G. M., Mentz, R. J., Cole, R. T., Adams, K. F., Egnaczyk, G. F., Fiuzat, M., et al. (2017). Efficacy and safety of tolvaptan in patients hospitalized with acute heart failure. *J. Am. Coll. Cardiol.* 69, 1399–1406. doi: 10.1016/j.jacc.2016.09.004
- Ghali, J. K., Hamad, B., Yasothan, U., and Kirkpatrick, P. (2009). Tolvaptan. *Nat. Rev. Drug Discov.* 8, 611–612. doi: 10.1038/nrd2946
- Gralla, R. J., Ahmad, F., Blais, J. D., Chiodo, J., Zhou, W., Glaser, L. A., et al. (2017). Tolvaptan use in cancer patients with hyponatremia due to the syndrome of inappropriate antidiuretic syndrome: a post hoc analysis of the SALT-1 and SALT-2 trials. *Cancer Med.* 6, 723–729. doi: 10.1002/cam4.805
- Graziani, G., Cucchiari, D., Aroldi, A., Angelini, C., Gaetani, P., and Selmi, C. (2012). Syndrome of inappropriate secretion of antidiuretic hormone in traumatic brain injury: when tolvaptan becomes a life saving drug. *J. Neurol. Neurosurg. Psychiatr.* 83, 510–512. doi: 10.1136/jnnp-2011-300576
- Hsu, H. T., Tseng, Y. T., Lo, Y. C., and Wu, S. N. (2014). Ability of naringenin, a bioflavonoid, to activate M-type potassium current in motor neuron-like cells and to increase BKCa-channel activity in HEK293T cells transfected with α -Slo subunit. *BMC Neurosci.* 15, 135. doi: 10.1186/s12868-014-0135-1
- Ichimura, S., Fahlbusch, R., and Lüdemann, W. (2015). Treatment of hyponatremia with tolvaptan in a patient after neurosurgical treatment of a pituitary tumor: case report and review of literature. *J. Neurol. Surg. Rep.* 76, e279–e281. doi: 10.1055/s-0035-1564605
- Iijima, M., Yoshimizu, T., Shimazaki, T., Tokugawa, K., Fukumoto, K., Kurosu, S., et al. (2014). Antidepressant and anxiolytic profiles of newly synthesized arginine vasopressin V1B receptor antagonists: TASP0233278 and TASP0390325. *Br. J. Pharmacol.* 171, 3511–3525. doi: 10.1111/bph.12699
- Imamura, T., and Kinugawa, K. (2018). Update of acute and long-term tolvaptan therapy. *J. Cardiol.* 73, 102–107. doi: 10.1016/j.jcc.2018.10.003
- Izumi, Y., Miura, K., and Iwao, H. (2014). Therapeutic potential of vasopressin-receptor antagonists in heart failure. *J. Pharmacol. Sci.* 124, 1–6. doi: 10.1254/jphs.13R13CP
- Jan, C. R., Wu, S. N., and Tseng, C. J. (1999). The ether lipid ET-18-OCH3 increases cytosolic Ca²⁺ concentrations in Madin Darby canine kidney cells. *Br. J. Pharmacol.* 127, 1502–1510. doi: 10.1038/sj.bjp.0702691
- Jannek, M., Burkhardt, T., Rotermund, R., Sauer, N., Flitsch, J., and Aberle, J. (2014). Hyponatremia after trans-sphenoidal surgery. *Minerva Endocrinol.* 39, 27–31.
- Jespersen, T., Rasmussen, H. B., Grunnet, M., Jensen, H. S., Angelo, K., Dupuis, D. S., et al. (2004). Basolateral localization of KCNQ1 potassium channels in MDCK cells: molecular identification of an N-terminal targeting motif. *J. Cell Sci.* 117, 4517–4526. doi: 10.1242/jcs.01318
- Kato, M., Tohyama, K., Ohya, T., Hiro, T., and Hirayama, A. (2016). Association between plasma concentration of tolvaptan and urine volume in acute decompensated heart failure patients with fluid overload. *Cardiol. J.* 23, 497–504. doi: 10.5603/CJ.a2016.0055
- Kogure, T., Jujo, K., Hamada, K., Saito, K., and Hagiwara, N. (2018). Good response to tolvaptan shortens hospitalization in patients with congestive heart failure. *Heart Vessels* 33, 374–383. doi: 10.1007/s00380-017-1072-6
- Konstam, M. A., Kiernan, M., Chandler, A., Dhingra, R., Mody, F. V., Eisen, H., et al. (2017). SECRET of CHF investigators, coordinators, and committee members. *J. Am. Coll. Cardiol.* 69, 1409–1419. doi: 10.1016/j.jacc.2016.12.035
- Lang, F., and Paulmichi, M. (1995). Properties and regulation of ion channels in MDCK cells. *Kidney Int.* 48, 1200–1205. doi: 10.1038/ki.1995.403
- Liu, J. W., and Ben-Jonathan, N. (1994). Prolactin-releasing activity of neurohypophysial hormones: structure-function relationship. *Endocrinology* 134, 114–118. doi: 10.1210/endo.134.1.8275925
- Liu, Y. C., Wang, Y. J., Wu, P. Y., and Wu, S. N. (2009). Tramadol-induced block of hyperpolarization-activated cation current in pituitary lactotrophs. *Naunyn Schmiedeberg Arch. Pharmacol.* 379, 127–135. doi: 10.1007/s00210-008-0353-0
- Mancinelli, R., Franchitto, A., Glaser, S., Vetuschi, A., Venter, J., Sferra, R., et al. (2016). Vasopressin regulates the growth of the biliary epithelium in polycystic liver disease. *Lab. Invest.* 96, 1147–1155. doi: 10.1038/labinvest.2016.93
- Matsukawa, R., Kubota, T., Okabe, M., Yamamoto, Y., and Meno, H. (2018). Efficacy and safety of the early use of V2 receptor antagonists in elderly

- patients with decompensated heart failure. *Heart Vessels* 33, 145–154. doi: 10.1007/s00380-017-1039-7
- McEwan, P., Bennett Wilton, H., Ong, A. C. M., Ørskov, B., Sandford, R., Scolari, F., et al. (2018). A model to predict disease progression in patients with autosomal dominant polycystic kidney disease (ADPKD): the ADPKD outcomes model. *BMC Nephrol.* 19:37. doi: 10.1186/s12882-017-0804-2
- Morris, J. H., Bohm, N. M., Nemecek, B. D., Crawford, R., Kelley, D., Bhasin, B., et al. (2018). Rapidity of correction of hyponatremia due to syndrome of inappropriate secretion of antidiuretic hormone following tolvaptan. *Am. J. Kidney Dis.* 71, 772–782. doi: 10.1053/j.ajkd.2017.12.002
- Müller, R. U., Haas, C. S., and Sayer, J. A. (2018). Practical approaches to the management of autosomal dominant polycystic kidney disease patients in the era of tolvaptan. *Clin. Kidney J.* 11, 62–69. doi: 10.1093/ckj/sfx071
- Nakajima, T., Hazama, H., Hamada, E., Wu, S. N., Igarashi, K., Yamashita, T., et al. (1996). Endothelin-1 and vasopressin activated Ca²⁺-permeable non-selective cation channels in aortic smooth muscle cells: mechanism of receptor-mediated Ca²⁺ influx. *J. Mol. Cell. Cardiol.* 28, 707–722. doi: 10.1006/jmcc.1996.0066
- Oguri, M., Ishii, H., Ohguchi, S., Takahara, K., Kawamura, Y., Yokoi, Y., et al. (2018a). Comparison of two dosing methods for immediate administration of tolvaptan in acute decompensated heart failure. *J. Cardiol.* 72, 234–239. doi: 10.1016/j.jicc.2018.02.006
- Oguro, M., Kogure, Y., Hoshino, J., Ubara, Y., Mizuno, H., Sekine, A., et al. (2018b). Tolvaptan in Japanese patients with later-stage autosomal dominant polycystic kidney disease. *J. Nephrol.* 31, 961–966. doi: 10.1007/s40620-018-0545-8
- Poch, E., Rodas, L., Blasco, M., Molina, A., and Quintana, L. (2018). An update on tolvaptan for autosomal dominant polycystic kidney disease. *Drugs Today* 54, 519–533. doi: 10.1358/dot.2017.54.9.2776624
- Quintero, J. L., Arenas, M. I., and García, D. E. (2005). The antidepressant imipramine inhibits M current by activating a phosphatidylinositol 4,5-bisphosphate (PIP₂)-dependent pathway in rat sympathetic neurons. *Br. J. Pharmacol.* 145, 837–843. doi: 10.1038/sj.bjp.0706239
- Rahman, S., and Rahman, T. (2017). Unveiling some FDA-approved drugs as inhibitors of the store-operated Ca²⁺ entry pathway. *Sci. Rep.* 7:12881. doi: 10.1038/s41598-017-13343-x
- Romanelli, N., Sartiani, L., Masi, A., Mannaioni, G., Manetti, D., Mugelli, A., et al. (2016). HCN channel modulators: the need for selectivity. *Curr. Top. Med. Chem.* 16, 1764–1791. doi: 10.2174/1568026616999160315130832
- Rudy, B., and McBain, C. J. (2001). Kv3 channels: voltage-gated K⁺ channels designed for high-frequency repetitive firing. *Trends Neurosci.* 24, 517–526. doi: 10.1016/S0166-2236(00)01892-0
- Sankaranarayanan, S., and Simasko, S. M. (1996). Characterization of an M-like current modulated by thyrotropin-releasing hormone in normal rat lactotrophs. *J. Neurosci.* 16, 1668–1678. doi: 10.1523/JNEUROSCI.16-05-01668.1996
- Sen, J., Chung, E., and McGill, D. (2018). Tolvaptan for heart failure in chronic kidney disease patients: a systemic review and meta-analysis. *Heart Lung Circ.* 27, 928–939. doi: 10.1016/j.hlc.2017.12.013
- Shoaf, S. E., Wang, Z., Bricmont, P., and Mallikaarjun, S. (2007). Pharmacokinetics, pharmacodynamics, and safety of tolvaptan, a nonpeptide AVP antagonist, during ascending single-dose studies in healthy subjects. *J. Clin. Pharmacol.* 47, 1498–1507. doi: 10.1177/0091270007307877
- Shu, Y., Yu, Y., Yang, J., and McCormick, D. A. (2007). Selective control of cortical axonal spikes by a slowly inactivating K⁺ current. *Proc. Natl. Acad. Sci. U.S.A.* 104, 11453–11458. doi: 10.1073/pnas.0702041104
- Sigal, S. H., Amin, A., Chiodo, J. A., and Sanyal, A. (2018). Management strategies and outcomes for hyponatremia in cirrhosis in the hyponatremia registry. *Can. J. Gastroenterol. Hepatol.* 2018:1579508. doi: 10.1155/2018/1579508
- So, E. C., Wang, Y., Yang, L. Q., So, K. H., Lo, Y. C., and Wu, S. N. (2018). Multiple regulatory actions of 2-guanidine-4-methylquinazoline (GMQ), an agonist of acid-sensing ion channel type 3, on ionic currents in pituitary GH3 cells and in olfactory sensory (Rolf B1.T) neurons. *Biochem. Pharmacol.* 151, 79–88. doi: 10.1016/j.bcp.2018.02.027
- So, E. C., Wu, S. N., Wu, P. C., Chen, H. Z., and Yang, C. J. (2017). Synergistic inhibition of delayed rectifier K⁺ and voltage-gated Na⁺ currents by artemisinin in pituitary tumor (GH3) cells. *Cell. Physiol. Biochem.* 41, 2053–2066. doi: 10.1159/000475436
- Soiza, R. L., and Talbot, H. S. (2011). Management of hyponatremia in older people: old threats and new opportunities. *Ther. Adv. Drug Saf.* 2, 9–17. doi: 10.1177/2042098610394233
- Sweeney, W. E., and Avner, E. D. (2017). Emerging therapies for childhood polycystic kidney disease. *Front Pediatr* 5:77. doi: 10.3389/fped.2017.00077
- Tabata, H., Yoneda, T., Oshitari, T., Takahashi, H., and Natsugari, H. (2017). Tolvaptan-type vasopressin receptor ligands: important role of axial chirality in the active form. *J. Med. Chem.* 60, 4503–4509. doi: 10.1021/acs.jmedchem.7b00422
- Takimura, H., Hada, T., Kawano, M., Yabe, T., Takimura, Y., Nishio, S., et al. (2018). A novel validated method for predicting the risk of re-hospitalization for worsening heart failure and the effectiveness of the diuretic upgrading therapy with tolvaptan. *PLoS ONE* 13:e0207481. doi: 10.1371/journal.pone.0207481
- Tamma, G., Di Mise, A., Ranieri, M., Geller, A., Tamma, R., Zallone, A., et al. (2017). The V2 receptor antagonist tolvaptan raises cytosolic calcium and prevents AQP2 trafficking and function: an intro and *in vivo* assessment. *J. Cell. Mol. Med.* 21, 1767–1780. doi: 10.1111/jcmm.13098
- Tateno, T., and Robinson, H. P. (2007). Quantifying noise-induced stability of a cortical fast-spiking cell model with Kv3-channel-like current. *BioSystems* 89, 110–116. doi: 10.1016/j.biosystems.2006.05.016
- Torres, V. E., Chapman, A. B., Devuyt, O., Gansevoort, R. T., Perrone, R. D., Koch, G., et al. (2017). REPRISÉ trial investigators. Tolvaptan in later-stage autosomal dominant polycystic kidney disease. *N. Engl. J. Med.* 377, 1930–1942. doi: 10.1056/NEJMoa1710030
- van Gastel, M. D. A., and Torres, V. E. (2017). Polycystic kidney disease and the vasopressin pathway. *Ann. Nutr. Metab.* 70 (Suppl. 1), 43–50. doi: 10.1159/000463063
- Verbalis, J. G., Ellison, H., Hobart, M., Krasa, H., Ouyang, J., and Czerwiec, F. S. (2016). Tolvaptan and neurocognitive function in mild to moderate chronic hyponatremia: a randomized trial (INSIGHT). *Am. J. Kidney Dis.* 67, 893–901. doi: 10.1053/j.ajkd.2015.12.024
- Vidic, A., Shuster, J. E., Goff, Z. D., Godishala, A., Joseph, S. M., Chibnall, J. T., et al. (2019). Vasopressin antagonism for decompensated right-sided heart failure. *Int. J. Cardiol.* 274, 245–247. doi: 10.1016/j.ijcard.2018.08.036
- Wang, Y. J., Lin, M. W., Lin, A. A., Peng, H., and Wu, S. N. (2008). Evidence for state-dependent block of DPI 201-106, a synthetic inhibitor of Na⁺ channel inactivation, on delayed-rectifier K⁺ current in pituitary tumor (GH3) cells. *J. Physiol. Pharmacol.* 59, 409–423.
- Wu, M. Y., Chen, T. T., Chen, Y. C., Tarnag, D. C., Wu, Y. C., Lin, H. H., et al. (2017a). Effects and safety of oral tolvaptan in patients with congestive heart failure: a systematic review and network meta-analysis. *PLoS ONE* 12:e0184380. doi: 10.1371/journal.pone.0184380
- Wu, S. N., Chen, H. Z., Chou, Y. H., Huang, Y. M., and Lo, Y. C. (2015). Inhibitory actions by ibandronate sodium, a nitrogen-containing bisphosphonate, on calcium-activated potassium channels in Madin-Darby canine kidney cells. *Toxicol. Rep.* 2, 1182–1193. doi: 10.1016/j.toxrep.2015.08.010
- Wu, S. N., Chern, J. H., Shen, S., Chen, H. H., Hsu, Y. T., Lee, C. C., et al. (2017b). Stimulatory actions of a novel thiourea derivative on large-conductance, calcium-activated potassium channels. *J. Cell. Physiol.* 232, 3409–3421. doi: 10.1002/jcp.25788
- Wu, S. N., Hsu, M. C., Liao, Y. K., Wu, F. T., Jong, Y. J., and Lo, Y. C. (2012a). Evidence for inhibitory effect of flupirtine, a centrally acting analgesic, on delayed rectifier K⁺ currents in motor neuron-like cells. *Evid. Based Complement. Alternat. Med.* 2012:148403. doi: 10.1155/2012/148403
- Wu, S. N., Liu, S. I., and Huang, M. H. (2004). Cilostazol, an inhibitor of type 3 phosphodiesterase, stimulates large-conductance, calcium-activated potassium channels in pituitary GH3 cells and pheochromocytoma PC12 cells. *Endocrinology* 145, 1175–1184. doi: 10.1210/en.2003-1430
- Wu, S. N., Yang, W. H., Yeh, C. C., and Huang, H. C. (2012b). The inhibition by di(2-ethylhexyl)-phthalate of erg-mediated K⁺ current in pituitary

- tumor (GH3) cells. *Arch. Toxicol.* 86, 713–723. doi: 10.1007/s00204-012-0805-7
- Wu, S. N., Yeh, C. C., Huang, H. C., So, E. C., and Lo, Y. C. (2012c). Electrophysiological characterization of sodium-activated potassium channels in NG108-15 and NSC-34 motor neuron-like cells. *Acta Physiol.* 206, 120–134. doi: 10.1111/j.1748-1716.2012.02438.x
- Zhou, J., Augelli-Szafran, C. E., Bradley, J. A., Chen, X., Koci, B. J., Volberg, W. A., et al. (2005). Novel potent human ether-a-go-go-related gene (hERG) potassium channel enhancers and their *in vitro* antiarrhythmic activity. *Mol. Pharmacol.* 68, 876–884. doi: 10.1124/mol.105.014035

Conflict of Interest Statement: The authors declare that the research was conducted in the absence of any commercial or financial relationships that could be construed as a potential conflict of interest.

Copyright © 2019 Lu, Chang, Chan and Wu. This is an open-access article distributed under the terms of the Creative Commons Attribution License (CC BY). The use, distribution or reproduction in other forums is permitted, provided the original author(s) and the copyright owner(s) are credited and that the original publication in this journal is cited, in accordance with accepted academic practice. No use, distribution or reproduction is permitted which does not comply with these terms.